arXiv:0708.2782v2 [cond-mat.supr-con] 12 Jul 2010

Anisotropic quasiparticle scattering rates in slightly underdoped to optimally doped high-temperature $La_{2-x}Sr_xCuO_4$ superconductors

J. Chang,[1] M. Shi,[2] S. Pailhés,[1] M. Månsson,[3] T. Claesson,[3] O. Tjernberg,[3] A. Bendounan,[1] Y. Sassa,[1] L. Patthey,[2] N. Momono,[4] M. Oda,[4] M. Ido,[4] S. Guerrero,[5] C. Mudry,[5] and J. Mesot[1,6,*]

[1]*Laboratory for Neutron Scattering, ETH Zurich and Paul Scherrer Institute, CH-5232 Villigen PSI, Switzerland*
[2]*Swiss Light Source, Paul Scherrer Institute, CH-5232 Villigen PSI, Switzerland*
[3]*Materials Physics, Royal Institute of Technology KTH, S-164 40 Kista, Sweden*
[4]*Department of Physics, Hokkaido University - Sapporo 060-0810, Japan*
[5]*Condensed Matter Theory Group, Paul Scherrer Institute, CH-5232 Villigen PSI, Switzerland*
[6]*Institut de la materière complexe, Ecole Polytechnique Fedédérale de Lausanne (EPFL), CH-1015 Lausanne, Switzerland*

(Dated: July 13, 2010)

An angle-resolved photoemission study of the scattering rate in the superconducting phase of the high-temperature superconductor $La_{2-x}Sr_xCuO_4$ with $x = 0.145$ and $x = 0.17$, as a function of binding energy and momentum, is presented. We observe that the scattering rate scales linearly with binding energy up to the high-energy scale $E_1 \sim 0.4$ eV. The scattering rate is found to be strongly anisotropic, with a minimum along the (0,0)-(π,π) direction. A possible connection to a quantum-critical point is discussed.

I. INTRODUCTION

Angle-resolved photoelectron spectroscopy (ARPES) is a powerful probe of electronic interactions in solids. For example, in studies of high-temperature superconductors (HTSC), a low-energy kink, herein denoted E_0, was observed in the (0,0) to (π,π) direction (nodal direction) of the quasi-particle (QP) spectra.[1,2] Recently, the high-energy part (0.2-1.5 eV) of the ARPES spectra has attracted considerable attention[3–9]. Graf *et al.*[3] reported the existence of two high-energy anomalies E_1 and E_2 in the nodal dispersion. These three anomalies, in the nodal spectra, $E_0 \approx 0.06$ eV, $E_1 \approx 0.4$ eV, and $E_2 \approx 0.8$ eV seem to be universal for the cuprates and they have been interpreted in terms of many-body interactions.[10–15] We have shown in Ref. 6 that the high-energy anomaly E_1 exists throughout the whole Brillouin zone (BZ) and that E_1 disperses continuously as one moves from the nodal to the antinodal [(0,0)-$(\pi,0)$] direction.

Transport measurements have revealed anomalous normal-state (NS) properties of optimally doped HTSCs. The NS resistivity, at optimal doping, is found to scale linearly with the temperature T up to $T \sim 1000$ K.[16] This part of the phasediagram is therefore also known as the strange metal phase. Although anomalous NS properties have been described successfully by the marginal Fermi liquid (MFL) phenomenology,[17] there is still no consensus for the underlying interactions responsible for HTSC and these anomalous properties.

In this letter, we investigate the QP scattering rate in $La_{2-x}Sr_xCuO_4$(LSCO) close to optimally doping. Our main findings, valid for energies much larger than the superconducting gap, are twofold. First, the dominant scattering channel scales linearly with the binding energy ω. Second, this scattering channel is highly anisotropic, exhibiting a sharp minimum along the nodal direction. We emphasize that while these results do not elucidate the pairing mechanism of HTSC, they provide constrains to any theory of the strange metal phase.

II. METHODS

Single crystals LSCO with $x = 0.145$ and $x = 0.17$ were grown using the travelling solvent floating zone method.[18] Both samples have a transition temperature $T_c \approx 36$ K with $\Delta T_c \approx 1.5$ K. The ARPES experiments were performed on the Surface/Interface Spectroscopy (SIS) beamline at the Swiss Light Source of the Paul Scherrer Institute. The spectra were acquired with a SCIENTA SES2002 electron analyzer, which was calibrated by recording spectra from polycrystalline copper on the sample holder. The measurements were performed at $T = 15$ K under ultra-high vacuum using 55 eV circularly polarized photons with an energy resolution of 17-40 meV. Data were recorded in the 2nd BZ, but are presented in the 1st BZ, for convenience.

III. RESULTS

Starting with the low-energy properties, we plot in Figs. 1(a) and (b) the ARPES intensity as a function of binding-energy and electron momentum $\mathbf{k}$, along cuts through the nodal and anti-nodal points, respectively. The nodal spectrum is characterized by sharp peaks and the leading edge of the energy distribution curve (EDC) at $\mathbf{k}_F$ reaches the Fermi level E_F. The MDC linewidth are much broader in the anti-nodal spectrum and the leading edge of the EDCs at $\mathbf{k}_F$ is shifted away from E_F due to the presence of an energy gap Δ.[19] The double peak structure of anti-nodal MDC linewidth stems from the cut crossing two branches of the QP dispersion.

In Fig. 2(a) we show the ARPES intensity up to very high binding energy for the nodal cut shown in the inset. The background was subtracted and the inten-

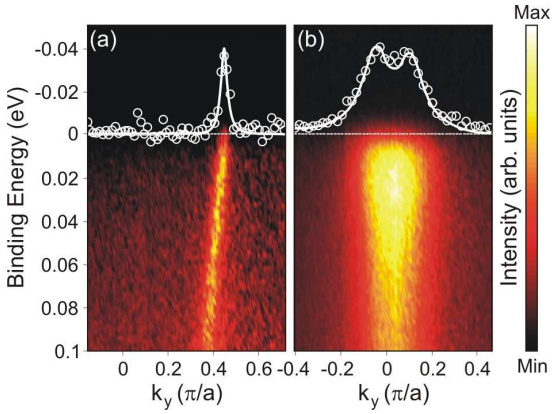

FIG. 1: (color) (a-b) ARPES intensity, recorded on $x = 0.145$, for nodal and anti-nodal cuts, respectively. The white points are the MDC at E_F. The intensity ratio between nodal and anti-nodal is $\sim 1/3$.

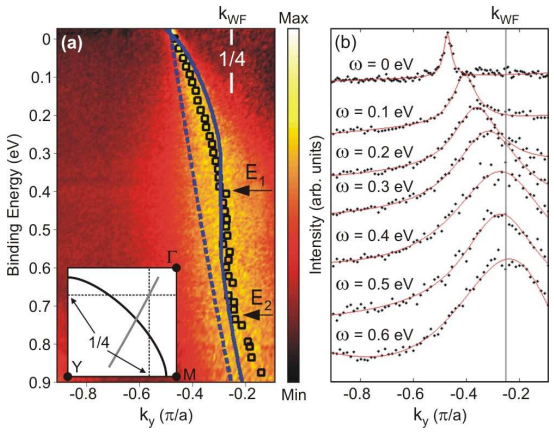

FIG. 2: (color) (a) MDC-normalized ARPES spectra, recorded on $x = 0.145$, for the nodal cut shown in the inset. Black squares represent the MDC peak-positions. Dashed blue line represents the bare band dispersion $\varepsilon_{\mathbf{k}}$. Solid blue line represents the renormalized dispersion obtained from discussions below. (b) MDCs for ω up to 0.6 eV. The red lines represents fits to the data with a Lorentzian lineshape on a sloping background.

sity was normalized to the maximum intensity of the momentum distribution curves (MDC) for each energy step. The open black squares indicate the dispersion extracted from MDC analysis according to Fig. 2(b) (the blue lines will be explained below). As previously reported,[3] the nodal spectrum exhibits two high-energy anomalies, E_1 and E_2, as indicated by black arrows in Fig. 2(a). For $E_1 < \omega < E_2$ the MDC peaks are pinned at $\mathbf{k}_{WF} \approx (1/4, 1/4)$, while for $\omega > E_2$ the MDC peaks disperse again. These anomalies have become known as the waterfall (WF) feature. Herein, the waterfall refers only to the $E_1(\phi_{WF})$ anomaly, and we use the notation $\mathbf{k}_{WF} = (|\mathbf{k}|, \phi)$, with the polar angle ϕ defined from the Y-point as shown in Fig. 3(c). This letter is dedicated to the study of the QP scattering rate $\mathrm{Im}\Sigma(\phi, \omega)$ that we model by assuming that it is the product of the MDC linewidth, $\Gamma(\phi, \omega)$, and a characteristic velocity $v(\phi)$, to be defined more precisely below. The polar angle ϕ is here, to a first approximation, labeling the cut along which the linewidth is measured. We limit our analysis to $\omega < 0.6$ eV where well-defined Lorentzian-shaped peaks, on nearly flat background, are observed in the MDC, as shown in Fig. 2(b). We examine the low- and high-energy dependence of the half-width at half-maximum (HWHM) $\Gamma(\phi, \omega)$ extracted from Lorentzian fits to the MDC from Fig. 3(a,d). The Fermi surfaces of LSCO with $x = 0.145$ and $x = 0.17$ shown in Figs. 3(b) and (c) respectively, are consistent with previous reports.[20] The color code of the cuts in Fig. 3(b,c) is the same as that in Fig. 3(a,d).

Before studying $\Gamma(\phi, \omega)$, we first discuss the ϕ-dependence of the high-energy anomaly E_1. Figure 4(a) shows E_1 extracted from the anomaly in the scattering rate shown in Fig. 3(d). $E_1(\phi_{WF})$ disperses strongly and we have previously suggested the following phenomenological form,

$$E_1(\phi_{WF}) = E_1(\pi/4)\left[1 - |\cos(2\phi_{WF})|\right] \qquad (1)$$

with $E_1(\pi/4) = 0.43$ eV.[6] Within the experimental uncertainty, there is no significant difference between $E_1(\phi_{WF})$ for LSCO with $x = 0.145$ and $x = 0.17$.

The energy scales E_0 and E_1 define three distinct characteristic regimes shown in Fig. 4(a). Regime I is the low-energy regime $E_F < \omega < \min\{E_0, E_1(\phi_{WF})\}$, followed by an intermediate regime II defined by $E_0 < \omega < E_1(\phi_{WF})$. Finally, we define the high-energy regime III by $E_1(\phi_{WF}) < \omega$.

Although the main purpose of this paper is to study the QP scattering rate $\Sigma(\phi, \omega)$ in regime II we present $\Gamma(\phi, \omega)$ in the three regimes. The MDC linewidth $\Gamma(\phi, \omega)$ in regimes I and II obey

$$\Gamma_i(\phi, \omega) = \Gamma_i^0(\phi) + \alpha_i(\phi)\omega, \qquad i = \mathrm{I,II}. \qquad (2)$$

Consistent with previous ARPES[21] and transport[22] measurements the elastic term $\Gamma_I^0(\phi_{FS})$ is anisotropic as shown in Fig. 4(b). The parameter $\alpha_I(\phi_{FS})$, related to the inelastic scattering, is analyzed by linear fits to the scattering rate $\Gamma_I(\phi_{FS}, \omega)$, see dashed lines in Fig. 3(a). We show in Fig. 4(c) the ϕ_{FS}-dependence of $\alpha_I(\phi_{FS})$ in the vicinity of the nodal point. The linear dependence of $\Gamma_I(\phi_{FS}, \omega)$ was also observed in Bi2212[23–25] and interpreted in ref.[25] as a signature of the d-wave nodes.

We now turn to regime II for which $\Gamma_{II}^0(\phi)$ is negligible for $x = 0.145$ and the angular dependence of $\alpha_{II}(\phi_{WF})$ is shown in Fig. 3(c). Observe that the coefficient α_{II} is the same for both $T_c > T = 15$ K and $T_c < T = 40$ K, see Fig. 3(d). This is expected since the relevant energy scale in regime II is an order of magnitude larger than the maximum of the superconducting gap. Hence the linear dependence on ω in Eq. (2) cannot be attributed to the d-wave nodes. Nevertheless and remarkably Γ_I^0, α_I, and α_{II}, follow a very similar angular dependence. To show this, we plot $\Gamma_0(\phi_{FS})/\Gamma_0(\pi/4)$, $\alpha_I(\phi_{FS})/\alpha_I(\pi/4)$ and

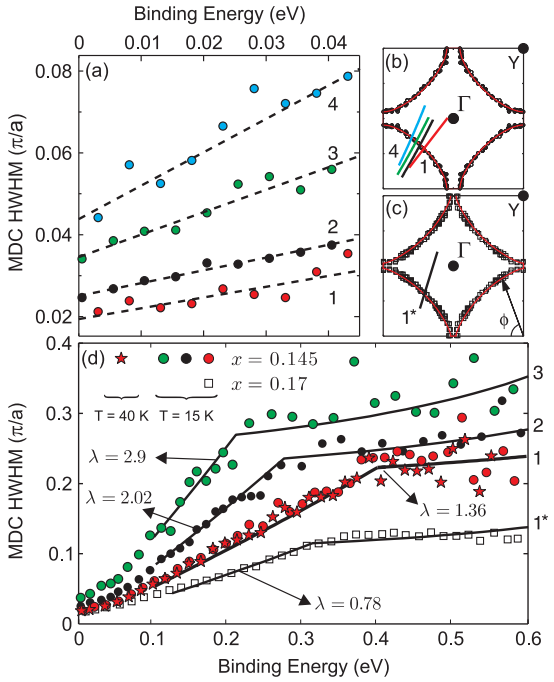

FIG. 3: (color) (a) Low-energy dependence of the MDC linewidths for the cuts shown in (b). Dashed lines represent linear fits of the measured scattering rate. (b-c) Fermi surface of $x = 0.145$ and $x = 0.17$ samples, respectively. The red lines are tight-binding fit to the data. (d) ω-dependence of MDC linewidth for cuts 1-3 in (b) and the cut in (c). Cut 1 in (b) was measured both in the SC state (circular points) and in the NS (star points) at $T = 40$ K. The solid lines are $\mathrm{Im}\Sigma(\omega)/v_\phi$ where $\mathrm{Im}\Sigma(\omega)$ and v_ϕ are given in the text.

$\alpha_{II}(\phi_{WF})/\alpha_{II}(\pi/4)$ in Fig. 4(d). For $La_{1.83}Sr_{0.17}CuO_4$ we find the same anisotropic dependence although with a slightly weaker and flatter dependence around the nodal direction, see Fig. 4(e).

The approximate Lorentzian shape of the MDCs suggests that one can neglect the $\mathbf{k}$- and ω-dependence of the photoelectron matrix elements. If so, we can approximate the ARPES intensity by the single-particle spectral function

$$A(\mathbf{k},\omega) = \frac{1}{\pi}\frac{-\mathrm{Im}\Sigma(\mathbf{k},\omega)}{\left[\omega - \mathrm{Re}\Sigma(\mathbf{k},\omega) - \varepsilon_{\mathbf{k}}\right]^2 + \left[\mathrm{Im}\Sigma(\mathbf{k},\omega)\right]^2}. \quad (3)$$

Here $\Sigma(\mathbf{k},\omega)$ is the self-energy and $\varepsilon_{\mathbf{k}}$ is the bare band dispersion. We model $\varepsilon_{\mathbf{k}}$ with the tight-binding dispersion

$$\begin{aligned}\varepsilon_{\mathbf{k}} = &-2t[\cos k_x a + \cos k_y a] - 4t' \cos k_x a \cos k_y a \\ &- 2t''[\cos 2k_x a + \cos 2k_y a] - \mu,\end{aligned} \quad (4)$$

where μ is the chemical potential, and t, t', and t'' denote nearest, second-nearest, and third-nearest neighbor hopping integrals on a square lattice, respectively. The ratios μ/t, t'/t, and t''/t, given in table I, are chosen such that $\varepsilon_{\mathbf{k}} = 0$ fits the experimentally determined Fermi surfaces, see Figs. 3(b) and (c). Assuming that the bandwidth t varies slowly within the doping range of interest, we use for the bare band $\varepsilon_{\mathbf{k}}$ (see dashed blue line in Fig. 2) $t = 0.48$ eV for both $x = 0.145$ and $x = 0.17$.[26]

In regime II we analyze the cuts shown in Fig. 3(b-c) with a generalized marginal Fermi liquid (MFL) self-energy

$$\mathrm{Im}\Sigma(\phi_{WF},\omega) = \frac{-\lambda(\phi_{WF})\pi}{2}\begin{cases}|\omega|, & |\omega| < \omega_c(\phi_{WF}),\\ \omega_c(\phi_{WF}), & |\omega| > \omega_c(\phi_{WF}),\end{cases} \quad (5)$$

and

$$\mathrm{Re}\Sigma(\phi_{WF},\omega) = -\lambda(\phi_{WF})\left[\omega \ln\left(\frac{\omega_c(\phi_{WF})}{\omega}\right) + ...\right]. \quad (6)$$

The conventional MFL ansatz[10,17] for the self-energy assumes that the dimensionless coupling λ and the characteristic energy cutoff ω_c are ϕ-independent. Motivated by Eqs. (2), we are going to relax this assumption in order to describe the MDC linewidth of Fig. 3 from Eqs. (3-6). Along the cuts shown in Fig. 3(b-c), the MDCs have a Lorentzian shape with HWHM $\Gamma(\phi,\omega) = \mathrm{Im}\Sigma(\phi,\omega)/v_\phi$ where $v_\phi = d\varepsilon_{\mathbf{k}}/d\mathbf{k}$ is the velocity along the cut.[27] Combining Eqs. (2) and (5), it then follows that

$$\pi\lambda(\phi_{WF}) = \alpha_{II}(\phi_{WF})v_\phi \approx \alpha_{II}(\phi_{WF})v_{\phi_{WF}}. \quad (7)$$

This approximation is valid in the vicinity of the nodal point where the bare-band velocity v_ϕ is weakly dependent on $\mathbf{k}$ for $\omega < 0.6$ eV but breaks down upon approaching the van Hove singularity of $\varepsilon_{\mathbf{k}}$ in the anti-nodal region. Second, we approximate the cutoff energy by

$$\omega_c(\phi_{WF}) \approx E_1(\phi_{WF}). \quad (8)$$

Now, the renormalized dispersion is the solution of $\omega_p(\mathbf{k}) = \mathrm{Re}\Sigma(\omega_p(\mathbf{k})) + \varepsilon_{\mathbf{k}}$. In this fashion we obtain a consistent agreement for both the renormalized dispersion [solid blue line in Fig. 2(a)] and the MDC linewidth [solid lines in Fig. 3(d)]. Thus, in contrast to earlier claims,[28] we have shown that the WF features can be described by a Kramers-Kronig consistent self-energy function $\Sigma(\phi,\omega)$. We would like to stress that the $\alpha_{II}(\phi_{WF})$ and $v_{\phi_{WF}}$ dependencies on ϕ_{WF} do not cancel out, leaving a net anisotropic coupling parameter $\lambda(\phi_{WF})$. Furthermore, the observation that $\alpha_{II}(\phi)$ has a stronger dependence on doping than $\varepsilon_{\mathbf{k}}$ implies that the coupling constant $\lambda(\phi_{WF})$ decreases with overdoping.

IV. DISCUSSION

We have shown that both the elastic and inelastic scattering rates are highly anisotropic. However, an isotropic channel may be hidden by the dominant anisotropic scattering channel. Recently, two scattering channels have been identified, in the overdoped regime of $Tl_2Ba_2CuO_{\delta+6}$ *(Tl2201)*, by an angular magnetoresistance oscillation (AMRO) study.[29] One channel, related to electron-electron scattering, is isotropic and exhibits T^2-dependence. A second channel, of unknown

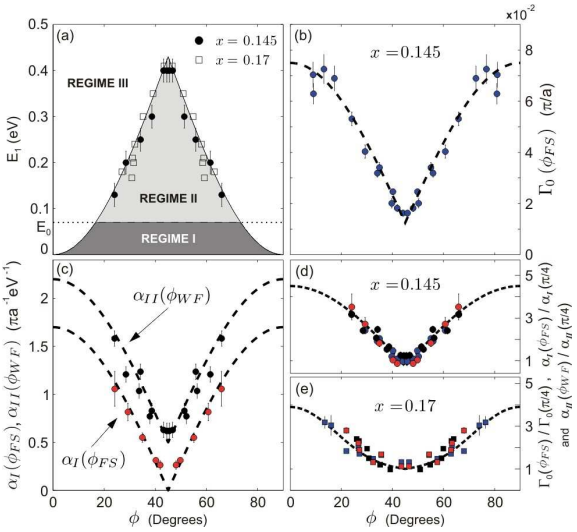

FIG. 4: (color) (a) Momentum dependence of E_1. Solid line is obtained from Eq. (1). (b) MDC linewidth Γ_0 as a function of the FS angle ϕ_{FS}. (c) Angular dependence of $\alpha_I(\phi)$ and $\alpha_{II}(\phi)$. (d-e) $\Gamma_0(\phi_{FS})/\Gamma_0(\pi/4)$, $\alpha_I(\phi_{FS})/\alpha_I(\pi/4)$ and $\alpha_{II}(\phi_{WF})/\alpha_{II}(\pi/4)$ for $x = 0.145$ and $x = 0.17$, respectively. Blue, red, and black points are Γ_0, α_I, and α_{II}, respectively. Data have been symmetrized with respect to the nodal direction. Dashed lines are guides to the eye.

TABLE I: Tight binding parameters for $La_{2-x}Sr_xCuO_4$.

Compound	t [eV]	μ/t	t'/t	t''/t	$E_1(\pi/4)/t$
$x = 0.145$	0.48	0.68	-0.125	0.078	0.9
$x = 0.17$	0.48	0.84	-0.144	0.072	0.9

origin, is anisotropic and depends linearly on T. For even more overdoped samples, resistivity measurements on $La_{2-x}Sr_xCuO_4$ have demonstrated that the electron-electron scattering channel is completely dominant.[29,30]

The picture that emerges from this work and previous transport measurements[29,30] is the following. In the underdoped regime the dominant scattering channel is highly anisotropic and exhibits MFL behavior. Upon further hole doping this channel gradually decreases and conventional electron-electron interactions become increasingly important. Eventually in the extremely overdoped regime, $x > 0.3$, electron-electron interactions are the dominant scattering mechanism.

V. CONCLUSION

In conclusion, we have presented a comprehensive study of the ω- and **k**-dependence of the scattering rate in the vicinity of optimally doped $La_{2-x}Sr_xCuO_4$. The dominant inelastic scattering channel scales linearly with ω up to the onset of the waterfall feature. Remarkably, both the elastic and inelastic scattering channels are strongly anisotropic, with minima along the nodal direction. This anisotropic MFL behavior can be used to discriminate between competing theories for the strange metallic phase in high-temperature superconductors that rely on the single-band Hubbard model,[31] the existence of a quantum critical point,[32–35] or the separation of spin and charge quantum numbers.[36,37]

VI. ACKNOWLEDGMENT

This work was supported by the Swiss NSF (through NCCR, MaNEP, and grant Nr 200020-105151), the Ministry of Education and Science of Japan and the Swedish Research Council. This work was performed at SLS of the Paul Scherrer Institute, Villigen PSI, Switzerland. We thank the beamline staff of X09LA for their excellent support and we are grateful to Lijun Zhu and Chandra Varma for enlightening discussions.

* Electronic address: joel.mesot@psi.ch

[1] A. Kaminski, J. Mesot, H. Fretwell, J. C. Campuzano, M. R. Norman, M. Randeria, H. Ding, T. Sato, T. Takahashi, T. Mochiku, K. Kadowaki, and H. Hoechst, Phys. Rev. Lett. **84**, 1788 (2000).

[2] A Lanzara, P.V. Bogdanov, X.J. Zhou, S.A. Kellar, D.L. Feng, E.D. Lu, T. Yoshida, H. Eisaki, A. Fujimori, K. Kishio, Shimoyama, T. Noda, S. Uchida, Z. Hussain, Z.X. Shen, Nature **412**, 510 (2001).

[3] J. Graf, G.-H. Gweon, K. McElroy, S. Y. Zhou, C. Jozwiak, E. Rotenberg, A. Bill, T. Sasagawa, H. Eisaki, S. Uchida, H. Takagi, D.-H. Lee and A. Lanzara, Phys. Rev. Lett. **98**, 067004 (2007).

[4] F. Ronning and K. M. Shen and N. P. Armitage and A. Damascelli and D. H. Lu and Z.-X. Shen and L. L. Miller and C. Kim, Phys. Rev. B **71**, 094518 (2005).

[5] B. P. Xie, K. Yang, D. W. Shen, J. F. Zhao, H. W. Ou, J. Wei, S. Y. Gu, M. Arita, S. Qiao, H. Namatame, M. Taniguchi, N. Kaneko, H. Eisaki, K. D. Tsuei, C. M. Cheng, I. Vobornik, J. Fujii, G. Rossi, Z. Q. Yang, and D. L. Feng, Phys. Rev. Lett. **98**, 147001 (2007).

[6] J. Chang, S. Pailhes, M. Shi, M. Maansson, T. Claesson, O. Tjernberg, J. Voigt, V. Perez, L. Patthey, N. Momono, M. Oda, M. Ido, A. Schnyder, C. Mudry, and J. Mesot, Phys. Rev. B **75**, 224508 (2007).

[7] Z.-H. Pan, P. Richard, A.V. Fedorov, T. Kondo, T. Takeuchi, S.L. Li, Pengcheng Dai, G.D. Gu, W. Ku, Z. Wang, and H. Ding, cond-mat/0610442 (2006).

[8] T. Valla and T. E. Kidd and W.-G. Yin and G. D. Gu and P. D. Johnson and Z.-H. Pan and A. V. Fedorov, Phys. Rev. Lett. **98**, 167003 (2007).

[9] W. Meevasana, X. J. Zhou, S. Sahrakorpi, W. S. Lee, W.

L. Yang, K. Tanaka, N. Mannella, T. Yoshida, D. H. Lu, Y. L. Chen, R. H. He, Hsin Lin, S. Komiya, Y. Ando, F. Zhou, W. X. Ti, J. W. Xiong, Z. X. Zhao, T. Sasagawa, T. Kakeshita, K. Fujita, S. Uchida, H. Eisaki, A. Fujimori, Z. Hussain, R. S. Markiewicz, A. Bansil, N. Nagaosa, J. Zaanen, T. P. Devereaux, and Z.-X. Shen, Phys. Rev. B **75**, 174506 (2007).

[10] Lijun Zhu and Vivek Aji and Arkady Shekhter and C. M. Varma, Phys. Rev. Lett. **100**, 057001 (2008).

[11] Efstratios Manousakis, Phys. Rev. B **75**, 035106 (2007).

[12] Fei Tan and Yuan Wan and Qiang-Hua Wang, Phys. Rev. B **76**, 54505 (2007).

[13] Alexandru Macridin and M. Jarrell and Thomas Maier and D. J. Scalapino Phys. Rev. Lett. **99**, 237001 (2007).

[14] R. S. Markiewicz and S. Sahrakorpi and A. Bansil, Phys. Rev. B **76**,174514 (2007).

[15] K. Byczuk and M. Kollar and K. Held and Y.F. Yang and I.A. Nekrasov and T. Pruschke and D. Vollhardt, Nat. Phys. **3**, 168 (2007).

[16] H. Takagi and B. Batlogg and H. L. Kao and J. Kwo and R. J. Cava and J. J. Krajewski and W. F. Peck, Jr., Phys. Rev. Lett. **69**, 2975 (1992).

[17] C. M. Varma and P. B. Littlewood and S. Schmitt-Rink, Phys. Rev. Lett. **63**, 1996 (1989).

[18] T. Nakano, N. Momono, M. Oda, and M. Ido, J. Phys. Soc. Jpn. **67**, 2622 (1998).

[19] M. Shi, J. Chang, S. Pailhes, M. R. Norman, J. C. Campuzano, M. Mnsson, T. Claesson, O. Tjernberg, A. Bendounan, L. Patthey, N. Momono, M. Oda, M. Ido, C. Mudry, and J. Mesot, Phys. Rev. Lett. **101**, 047002 (2008)

[20] T. Yoshida, X. J. Zhou, K. Tanaka, W. L. Yang, Z. Hussain, Z.-X. Shen, A. Fujimori, S. Sahrakorpi, M. Lindroos, R. S. Markiewicz, A. Bansil, Seiki Komiya, Yoichi Ando, H. Eisaki, T. Kakeshita, and S. Uchida, Phys. Rev. B **74**, 224510 (2006).

[21] T. Yoshida, X. J. Zhou, D. H. Lu, Seiki Komiya, Yoichi Ando, H. Eisaki, T. Kakeshita, S. Uchida, Z. Hussain, Z.-X. Shen, and A. Fujimori, J. Phys.: Condens. Matter **19**, 125209 (2007).

[22] A. Narduzzo, G. Albert, M. M. J. French, N. Mangkorntong, M. Nohara, H. Takagi and N. E. Hussey, Phys. Rev. B **77**, 220502 (2008)

[23] A. Kaminski, H. M. Fretwell, M. R. Norman, M. Randeria, S. Rosenkranz, U. Chatterjee, J. C. Campuzano, J. Mesot, T. Sato, T. Takahashi, T. Terashima, M. Takano, K. Kadowaki, Z. Z. Li, and H. Raffy, Phys. Rev. B **71**, 014517 (2005).

[24] T. Valla, T. E. Kidd, J. D. Rameau, H.-J. Noh, G. D. Gu, P. D. Johnson, H.-B. Yang, and H. Ding, Phys. Rev. B **73**, 184518 (2006).

[25] T. Yamasaki, K. Yamazaki, A. Ino, M. Arita, H. Namatame, M. Taniguchi, A. Fujimori, Z.-X. Shen, M. Ishikado, and S. Uchida, Phys. Rev. B **75**, 140513 (2007).

[26] E. Pavarini, I. Dasgupta, T. Saha-Dasgupta, O. Jepsen, and O. K. Andersen, Phys. Rev. Lett. **87**, 047003 (2001).

[27] T. Valla, A.V. Fedorov, P.D. Johnson, B.O. Wells, S.L. Hulbert, Q. Li, G.D. Gu, and N. Koshizuka, Science **285**, 2110 (1999).

[28] D. S. Inosov, J. Fink, A. A. Kordyuk, S. V. Borisenko, V. B. Zabolotnyy, R. Schuster, M. Knupfer, B. Bchner, R. Follath, H. A. Drr, W. Eberhardt, V. Hinkov, B. Keimer, and H. Berger, Phys. Rev. Lett., **99**, 237002 (2007), see also `cond-mat/0703223`.

[29] M. Abdel-Jawad, M.P. Kennett, L. Balicas, A. Carrington, A.P. Mackenzie, R.H. McKenzie, and N.E. Hussey, Nat. Phys. **2**, 821 (2006).

[30] S. Nakamae, K. Behnia, N. Mangkorntong, M. Nohara, H. Takagi, S. J. C. Yates, and N. E. Hussey, Phys. Rev. B 68, 100502(R) (2003)

[31] Y. Kakehashi and P. Fulde, Phys. Rev. Lett. **94**, 156401 (2005).

[32] C. M. Varma, Phys. Rev. Lett. **83**, 3538 (1999).

[33] Sudip Chakravarty, R. B. Laughlin, Dirk K. Morr and Chetan Nayak, Phys. Rev. B **63**, 094503 (2001)

[34] Eun-Ah Kim, Michael J. Lawler, Paul Oreto, Subir Sachdev, Eduardo Fradkin, and Steven A. Kivelson, Phys. Rev. B **77**, 184514 (2008)

[35] Andrea Pelissetto, Subir Sachdev and Ettore Vicari, Phys. Rev. Lett. **101**, 027005 (2008)

[36] P. A. Lee, N. Naogosa and X.-G Wen, Rev. Mod. Phys. **78**, 17 (2006).

[37] P.W. Anderson, Nat. Phys.**2**, 626-630 (2006).